Role of Volume Fraction of Reinforcement on Interfacial Debonding and Matrix Fracture in Titanium Carbide/AA4015 Alloy Particle-Reinforced Metal Matrix Composites

[1]S. Sundara Rajan and A. Chennakesava Reddy[2]

[1]Scientist-F, Defence Research and Development Organisation, Hyderabad, India.
[2]Assistant Professor, Department of Mechanical Engineering, MJ College of Engineering and Technology, Hyderabad, India
dr_acreddy@yahoo.com

Abstract: *A hexagonal array unit cell/ellipsoidal* TiC *nanoparticle RVE models were used to predict micromechanical behavior and interfacial debonding in AA4015/* TiC *composites. The AA4015/* TiC *particulate metal matrix composites were fabricated at different volume fractions of* TiC. *The stiffness of the composite has increased with increase of* TiC *volume fraction. The interfacial debonding and matrix fracture were observed in the composites.*

Keywords: AA4015*, titanium carbide, ellipsoidal nanoparticle, RVE model, finite element analysis, debonding.*

1. INTRODUCTION

In the micromechanics-based models, the damage evolution in composites can be described by transition of volume fraction from intact particles to damaged particles. As the fracture strength of brittle materials is higher when the size of reinforced particles is smaller, the fracture and debonding of particles in composites is harder to occur on smaller sized particles. Debonding of particles is controlled by a critical value of particle stress because the interfacial stress between particles and matrix is described as a function of the particle stress [1, 2]. A study was conducted on the silane interfacial effect on the fracture process of embedded single E-glass fiber [3]. The interfacial reinforcement reflects the progressed fracture rather than the instantaneous fracture. A variety of nanoparticles such as silicon nitride [4, 5], titanium oxide [6, 7], graphite [8], titanium carbide [9, 10], boron nitride [11], zirconium oxide [12], titanium nitride [13], titanium boride [14], zirconium carbide [15], silicon oxide [16], magnesium oxide [17] at 10%, 20% and 30% volume fractions were studied and the results computed from a unit cell with uniformly distributed particles were compared. The influence of progressive damage on stress-strain relation of particulate-reinforced composites was studied with two schemes. Finite element analysis for a unit cell containing one particle in a matrix was widely applied to fracture or debonding of particles [18]. The unit cell analysis has an advantage to provide details of damage process in one particle [4-17].

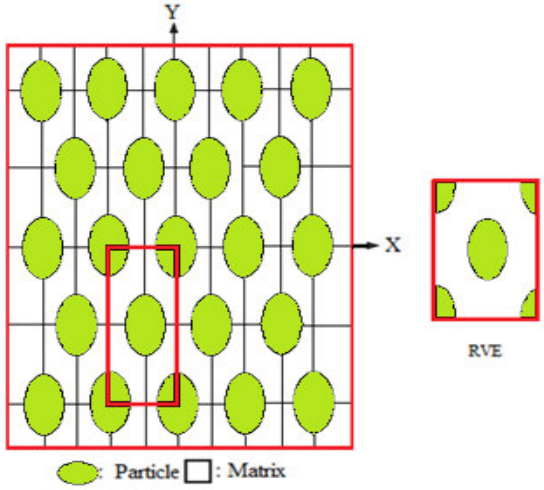

Figure 1: A diamond RVE containing an ellipsoidal nanoparticle.

High particle hardness and slick surfaces make titanium carbide (TiC) is an ideal filler material to enhance wear-resistant, tribological, and mechanical bearing characteristics. The shape of TiC particle considered in this work is a ellipsoidal. The periodic particle distribution was a hexagonal array as shown in figure 1.

2. THEORETICAL BACKGROUND

The strains along x- and y-directions can be determined as using the following equations:

$$\varepsilon_y = -\left(\frac{v_{xy}}{E_x} + \frac{1}{E_z}\right)P = \frac{\Delta y}{a} \quad (1)$$

$$\varepsilon_x = \left(\frac{1}{E_x} - \frac{1}{E_z}\right)P = \frac{\Delta x}{a} \quad (2)$$

The effective elastic moduli and Poisson's ratio in the transverse direction (xy-plane) as follows:

$$E_x = \frac{1}{\frac{\Delta x}{Pa} + \frac{1}{E_z}} \text{ and } E_y = \frac{1}{\frac{\Delta y}{Pa} + \frac{1}{E_z}} \quad (3)$$

$$v_{xy} = \left(\frac{\Delta y}{Pa} + \frac{1}{E_z}\right)/\left(\frac{\Delta x}{Pa} + \frac{1}{E_z}\right) \quad (4)$$

Once the change in lengths along x- and y- direction (Δx and Δy) are determined for the square RVE from the FEA, E_y and E_x and v_{xy} can be determined from Eqs. (3) and (4), correspondingly. Considering adhesion, formation of precipitates, particle size, agglomeration, voids/porosity, obstacles to the dislocation, and the interfacial reaction of the particle/matrix, the formula for the strength of composite is stated below:

$$\sigma_c = \left[\sigma_m \left\{\frac{1-(v_p+v_v)^{2/3}}{1-1.5(v_p+v_v)}\right\}\right] e^{m_p(v_p+v_v)} + k d_p^{-1/2} \quad (5)$$

$$k = E_m m_m / E_p m_p$$

where, v_v and v_p are the volume fractions of voids/porosity and nanoparticles in the composite respectively, m_p and m_m are the possion's ratios of the nanoparticles and matrix respectively, d_p is the mean nanoparticle size (diameter) and E_m and E_p is elastic moduli of the matrix and the particle respectively. Elastic modulus (Young's modulus) is a measure of the stiffness of a material and is a quantity used to characterize materials. Elastic modulus is the same in all orientations for isotropic materials. Anisotropy can be seen in many composites.

The upper-bound equation is given by

$$\frac{E_c}{E_m} = \left(\frac{1-v_v^{2/3}}{1-v_v^{2/3}+v_v}\right) + \frac{1+(\delta-1)v_p^{2/3}}{1+(\delta-1)(v_p^{2/3}-v_p)} \quad (6)$$

The lower-bound equation is given by

$$\frac{E_c}{E_m} = 1 + \frac{v_p - v_p}{\delta/(\delta-1)-(v_p+v_v)^{1/3}} \quad (7)$$

where, $\delta = E_p/E_m$.

The transverse modulus is given by

$$E_t = \frac{E_m E_p}{E_m + E_p(1-v_p^{2/3})/v_p^{2/3}} + E_m\left(1 - v_p^{2/3} - v_v^{2/3}\right) \quad (8)$$

3. MATERIALS METHODS

The matrix material was AA4015 alloy. The reinforcement material was ellipsoidal TiC nanoparticles of average size 100nm. The mechanical properties of materials used in the present work are given in table 1.

Table 1: Mechanical properties of AA4015 matrix and TiC nanoparticles

Property	AA4015	TiC
Density, g/cc	2.71	4.93
Elastic modulus, GPa	68.90	400.00
Ultimate tensile strength, MPa	155	119
Poisson's ratio	0.33	0.19

AA4015 alloy/TiC composites were manufactured by the stir casting process and low pressure casting technique with argon gas at 3.0 bar. The composite samples were give solution treatment and cold rolled to the predefined size of tensile specimens. The heat-treated samples were machined to get flat-rectangular specimens (figure 2) for the tensile tests. The tensile specimens were placed in the grips of a Universal Test Machine (UTM) at a specified grip separation and pulled until failure. The test speed was 2 mm/min (as for ASTM D3039). A strain gauge was used to determine elongation.

In this research, a cubical representative volume element (RVE) was implemented to analyze the tensile behavior AA4015/ TiC nanoparticle composites at three (10%, 20% and 30%) volume fractions of TiC. The large strain PLANE183 element was used

in the matrix in all the models. In order to model the adhesion between the matrix and the particle, a CONTACT 172 element was used.

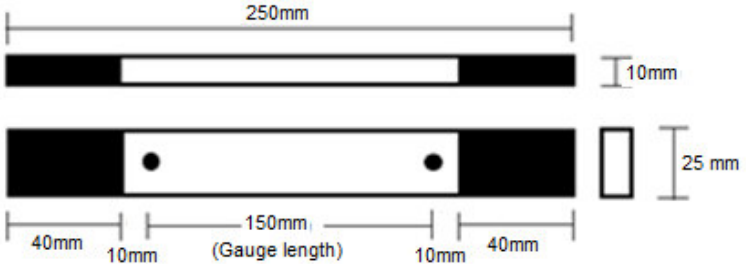

Figure 2: Shape and dimensions of tensile specimen

4. RESULTS AND DISCUSSION

The micromechanical behavior is discussed in terms of tensile elastic moduli, E_x, shear modulus, G_{xy} and major Poisson's ratio, v_{xy}. The fracture behavior is conversed in terms of interface debonding and particle fracture.

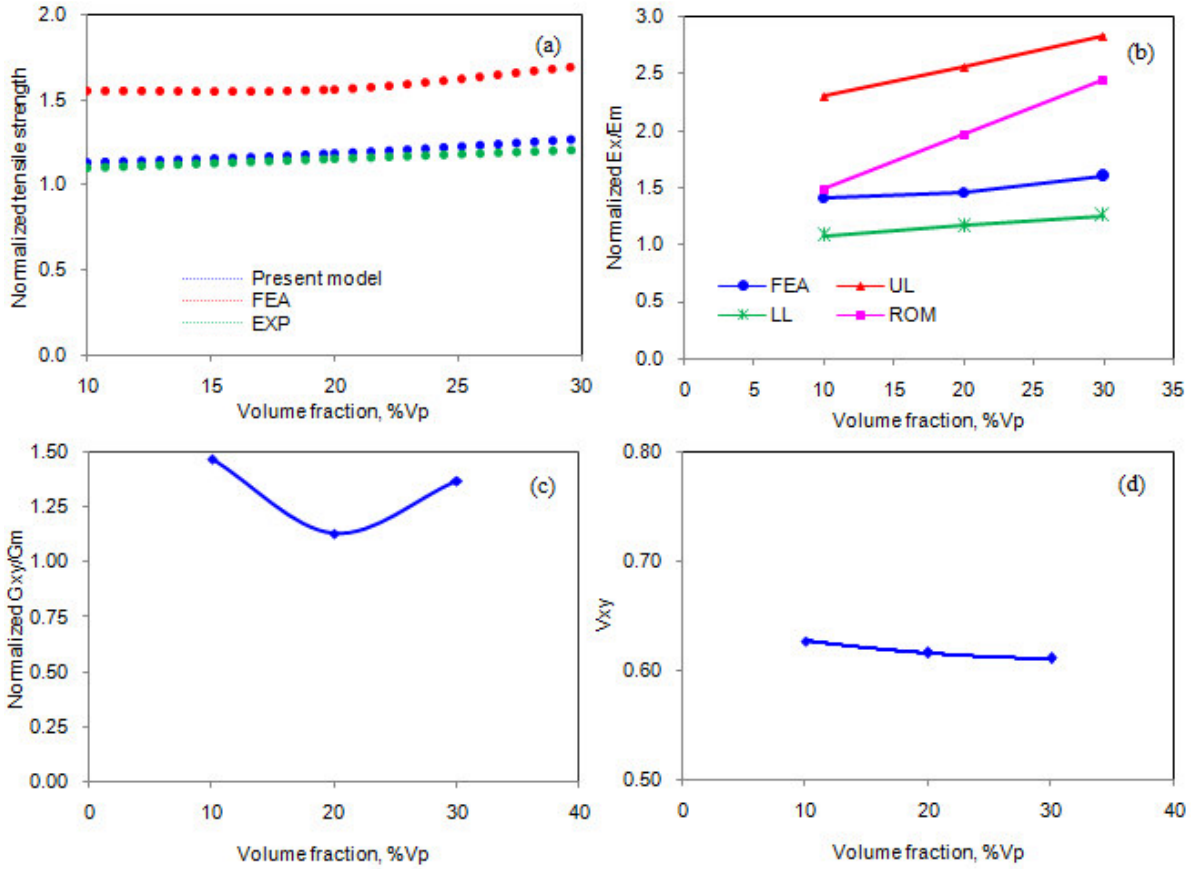

Figure 3: Effect of volume fraction on micromechanical behavior of AA4015/TiC composites.

4.1 Micromechanical Behavior

Figure 3a represents the normalized tensile strengths of the AA4015 alloy/ TiC composites obtained by FEA, present mathematical model, and experimental test. The tensile strength is normalized with ultimate tensile strength of AA4015 alloy. The results obtained from present mathematical model and the experimental procedures are approximately equal. The difference between the results obtained from experimental procedure and the FEA is due to the ignorance of porosity in the matrix, uniform distribution of TiC particles and agglomeration of TiC particles. The normalized elastic modulus is shown in figure 3b. The elastic modulus is normalized with the elastic modulus of AA4015 alloy. The stiffness of the composites increases with

increase of volume fraction of TiC. The upper limit (UL) values computed by the present mathematical model are higher than those values obtained by the 'Role of Mixtures (ROM)'and FEA. This is because of assumption of voids in the present mathematical model. The shear strength of the composites is low for the volume fraction of 20% TiC (figure 3c). The major Poisson's ratio decreases with increase of volume fraction of TiC particles (figure 3d).

4.2 Fracture Analysis

If the particle deforms in an elastic manner (according to Hooke's law) then,

$$\tau = \frac{n}{2}\sigma_p \quad (9)$$

where σ_p is the particle stress. If particle fracture occurs when the stress in the particle reaches its ultimate tensile strength, $\sigma_{p,uts}$, then setting the boundary condition at

$$\sigma_p = \sigma_{p,\,uts} \quad (10)$$

The relationship between the strength of the particle and the interfacial shear stress is such that if

$$\sigma_{P,uts} < \frac{2\tau}{n} \quad (11)$$

Then the particle will fracture. From the figure 4b, it is observed that the TiC nanoparticle was not fractured as the condition in Eq. (11) is not satisfied. For the interfacial debonding/yielding to occur, the interfacial shear stress reaches its shear strength:

$$\tau = \tau_{max} \quad (12)$$

For particle/matrix interfacial debonding can occur if the following condition is satisfied:

$$\tau_{max} < \frac{n\sigma_p}{2} \quad (13)$$

It is observed from figure 4a that the interfacial debonding occurs between TiC nanoparticle and AA4015 alloy matrix as the condition in Eq.(13) is satisfied.

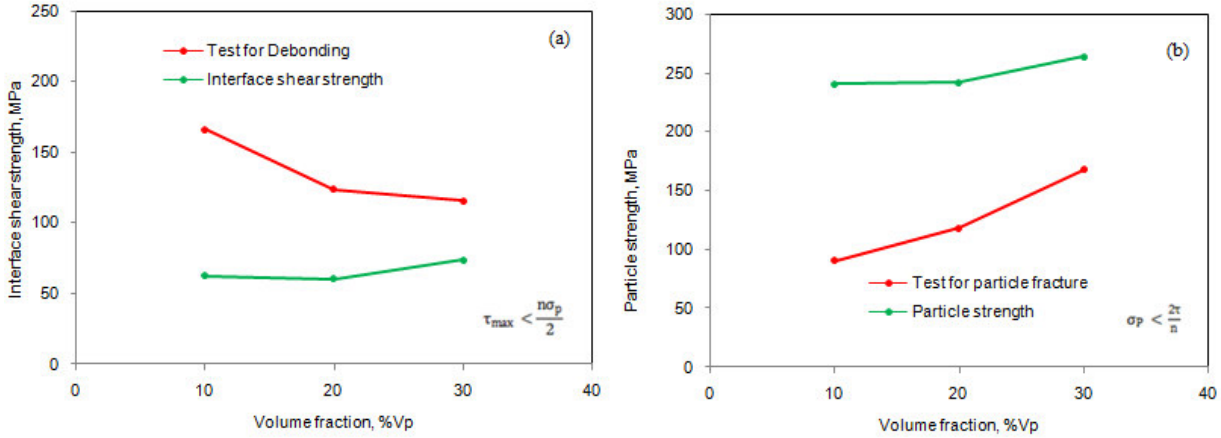

Figure 4: Criterion interfacial debonding (a) and for particle fracture (b).

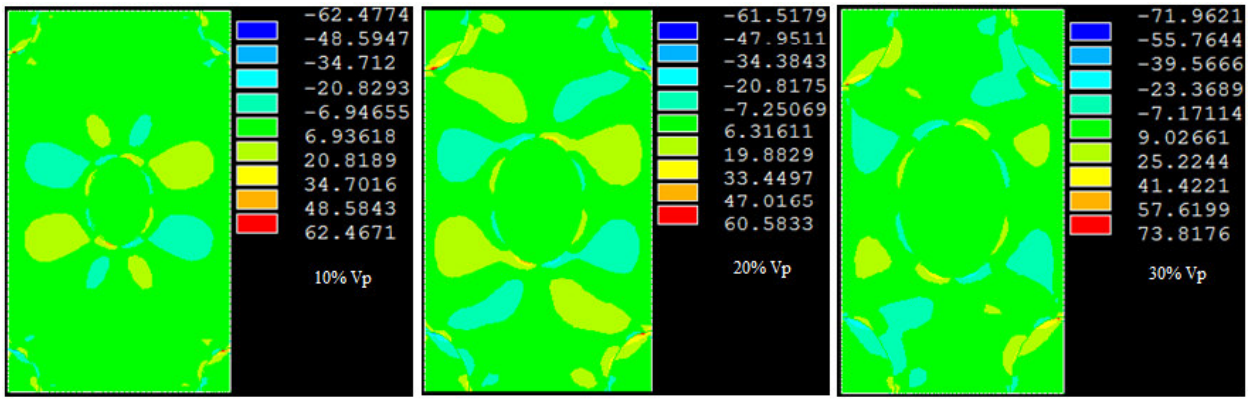

Figure 5: Images of tensile stress obtained from FEA.

As seen from 5 the shear stress developed at the interface are higher than that induced in the nanoparticle. Hence, the interfacial debonding was occurred between the particle and the matrix. The matrix fracture is also observed in AA4105/ TiC composites due to inadequate transfer of load from the matrix to the particle.

5. CONCLUSION

The shear stress is high at the interface leading to interfacial debonding in AA4015/ TiC composites. Due to lack of load transfer from the matrix to the particle, the fracture in the matrix is also observed. The stiffness of the composite increases with increase of TiC reinforced particle in the matrix of AA4015 alloy.

REFERENCES

1. G. P. Tandon, G. J. Weng, Stress distribution in and around spheroidal Inclusions and voids at finite concentration, ASME Journal of Applied Mechanics, 53, 1986, pp.511-518.
2. C. W. Nan, D. R. Clarke, The influence of particle size and particle fracture on the elastic/plastic deformation of metal matrix composites, Acta Materialia, 44, 1996, pp. 3801-3811.
3. B. Kotiveerachari, A. Chennakesava Reddy, Interfacial effect on the fracture mechanism in GFRP composites, CEMILAC Conference, Ministry of Defence, India, 20-21st August 1999.
4. A. Chennakesava Reddy, Assessment of Debonding and Particulate Fracture Occurrences in Circular Silicon Nitride Particulate/AA5050 Alloy Metal Matrix Composites , National Conference on Materials and Manufacturing Processes, Hyderabad, India, 27-28 February 1998, pp. 104-109.
5. A. Chennakesava Reddy, Evaluation of Debonding and Dislocation Occurrences in Rhombus Silicon Nitride Particulate/AA4015 Alloy Metal Matrix Composites, 1st National Conference on Modern Materials and Manufacturing , Pune, India, 19-20 December 1997, pp. 278-282.
6. S. Sundara Rajan, A. Chennakesava Reddy, Deformation Behavior of AA8090/ TiO_2 Nanoparticulate Reinforced Metal Matrix Composites with Debonding Interfaces, 2nd International Conference on Composite Materials and Characterization, Nagpur, India, 9-10 April 1999, pp. 245-248.
7. A. Chennakesava Reddy, Cohesive Zone Finite Element Analysis to Envisage Interface Debonding in AA7020/Titanium Oxide Nanoparticulate Metal Matrix Composites , 2nd International Conference on Composite Materials and Characterization, Nagpur, India, 9-10 April 1999, pp. 204-209.
8. A. Chennakesava Reddy, Micromechanical Modelling of Interfacial Debonding in AA1100/Graphite Nanoparticulate Reinforced Metal Matrix Composites, 2nd International Conference on Composite Materials and Characterization, Nagpur, India, 9-10 April 1999, pp. 249-253.
9. A. Chennakesava Reddy, Local Stress Differential for Particulate Fracture in AA2024/Titanium Carbide Nanoparticulate Metal Matrix Composites, National Conference on Materials and Manufacturing Processes, Hyderabad, India, 27-28 February 1998, pp. 127-131.
10. B. Kotiveera Chari, A. Chennakesava Reddy, Effect of Debonding on Overall Behavior of AA3003/Titanium Carbide Nanoparticulate Reinforced Metal Matrix Composites, 2nd International Conference on Composite Materials and Characterization, Nagpur, India, 9-10 April 1999, pp. 220-224.
11. H. B. Niranjan, A. Chennakesava Reddy, Effect of Particulate Debonding in AA5050/Boron Nitride Nanoparticulate Reinforced Metal Matrix Composites, 2nd International Conference on Composite Materials and Characterization, Nagpur, India, 9-10 April 1999, pp. 230-234.
12. P. M. Jebaraj, A. Chennakesava Reddy, Interface Debonding Prediction Technique for Tensile Loaded AA6061/Zirconium Oxide Nanoparticulate MMC, 2nd International Conference on Composite Materials and Characterization, Nagpur, India, 9-10 April 1999, pp. 235-239.
13. S. Sundara Rajan, A. Chennakesava Reddy, FEM Model for Volume Fraction Dependent Interface Debonding in TiN Nanoparticle Reinforced AA7020 Metal Matrix Composites, 2nd International Conference on Composite Materials and Characterization, Nagpur, India, 9-10 April 1999, pp. 240-244.
14. A. Chennakesava Reddy, Interfacial Debonding Analysis in Terms of Interfacial Tractions for Titanium Boride/AA3003 Alloy Metal Matrix Composites, 1st National Conference on Modern Materials and Manufacturing , Pune, India, 19-20 December 1997, pp. 124-127.
15. B. Kotiveera Chari, A. Chennakesava Reddy, Interfacial Debonding Analysis in Nanoparticulate Reinforced Metal Matrix Composites of AA8090/Zirconium Carbide, 2nd International Conference on Composite Materials and Characterization, Nagpur, India, 9-10 April 1999, pp. 210-214.
16. H. B. Niranjan, A. Chennakesava Reddy, Debonding Failure and Volume Fraction Effects in Nano-reinforced Composites of AA2024/Silicon Oxide, 2nd International Conference on Composite Materials and Characterization, Nagpur, India, 9-10 April 1999, pp. 215-219.
17. P. M. Jebaraj, A. Chennakesava Reddy, Analysis of Debonding along Interface of AA4015/Magnesium Oxide Nanoparticulate Reinforced Metal Matrix Composites, 2nd International Conference on Composite Materials and Characterization, Nagpur, India, 9-10 April 1999, pp. 225-229.
18. M. Finot, Y. L. Shen, A. Needleman, S. Suresh, Micromechanical modeling of reinforcement fracture in particle-reinforced metal-matrix composites, Metallurgical and Material Transaction, 25A, 1994, pp. 2403-2420.